Molecular Crystals and Liquid Crystals Science and Technology. Section A. Molecular Crystals and Liquid Crystals

Publication details, including instructions for authors and subscription information:
http://www.tandfonline.com/loi/gmcl19

Theory of Biexcitons in π-Conjugated Polymers

F. Guo [a], M. Chandross [a] & S. Mazumdar [a b]

[a] Department of Physics, University of Arizona, Tucson, AZ, 85721

[b] Optical Sciences Center, University of Arizona, Tucson, AZ, 85721

Version of record first published: 04 Oct 2006.

To cite this article: F. Guo , M. Chandross & S. Mazumdar (1994): Theory of Biexcitons in π-Conjugated Polymers, Molecular Crystals and Liquid Crystals Science and Technology. Section A. Molecular Crystals and Liquid Crystals, 256:1, 53-62

To link to this article: http://dx.doi.org/10.1080/10587259408039231

Mol. Cryst. Liq. Cryst. 1994, Vol. 256, pp. 53–62
Reprints available directly from the publisher
Photocopying permitted by license only

THEORY OF BIEXCITONS IN π–CONJUGATED POLYMERS

F. GUO[a], M. CHANDROSS[a], and S. MAZUMDAR[a,b]
[a]Department of Physics, University of Arizona, Tucson, AZ 85721
[b]Optical Sciences Center, University of Arizona, Tucson, AZ 85721

Abstract Theoretical models of π-conjugated polymers that emphasize the Coulomb electron-electron correlations predict that the lowest optical excitation is to an exciton. We have extended our theoretical studies to an energy region that is considerably higher, to probe specifically the states that are reached by two-electron excitations from the ground state. Theoretical evidence for the biexciton, a bound state of two excitons that occurs below the two-electron continuum, is found. The lowest biexciton state is of even parity, can be reached by optical excitation from the $1B_u$ exciton, and in principle also by two-photon excitation from the ground state. A high energy photoinduced absorption seen in the picosecond time domain in poly (*para*-phenylenevinylene) (PPV), as well as in other π-conjugated polymers, is interpreted as a transition from the exciton to the biexciton.

INTRODUCTION

It is becoming increasingly clear that the principal optical transition in π-conjugated polymers is not a band-to-band transition but an excitonic one. The exciton picture is most firmly established in the crystalline polydiacetylenes, where exciton binding energies of 0.5 eV and larger have been established[1]. More recently, the lowest optical transition in PPV has been shown to be excitonic[2]. Even in π-conjugated polymers in which the linear absorption resembles band-to-band transition, *nonlinear* spectra reveal the underlying excitonic spectrum. Thus the occurrence of three resonances in the third harmonic generation spectrum of cis-polyacetylene has been explained within the exciton picture[3]. In conventional semiconductors with large exciton binding energies (for e.g., CuCl with a binding energy of 200 meV), the biexciton concept is now firmly established[4]. Even larger binding energies in the π-conjugated polymers then strongly suggest stable biexcitons. In this context it is also perhaps relevant that stable multiexitons have very recently been demonstrated in a quasi-one-dimensional organic mixed-stack neutral charge-transfer (CT) solid[5]. The common feature among conjugated polymers and CT solids is quasi-one-dimensionality (and the resultant confinement effect), and the investigation of biexciton stability is clearly of interest. This is especially so in view of the recent controversy over the origin of the picosecond (ps) photoinduced absorption (PA) in the polymers, which has been explained both within the biexciton concept[6] and as transition within a polaron-pair state[7]. In the following we present

theoretical evidence for stable biexcitons within the extended Hubbard Hamiltonian, for realistic Coulomb interaction parameters. The underlying physical picture is the same as presented by us earlier for the nonresonant nonlinear optical properties of π-conjugated polymers[3,8]. Following this, we discuss PA in the experimental systems.

THEORETICAL MODEL

We use the extended Peierls-Hubbard Hamiltonian,

$$H = U\sum_i n_{i,\uparrow}n_{i,\downarrow} + V\sum_i (n_i - 1)(n_{i+1} - 1)$$

$$-t\sum_{i,\sigma}[1 - (-1)^i\delta][c^+_{i,\sigma}c_{i+1,\sigma} + c^+_{i+1,\sigma}c_{i,\sigma}] \quad (1)$$

Only the last term occurs in the Huckel model, to which we have added the on-site and nearest neighbor electron correlations, U and V. These two interactions can give all the novel physical effects that occur in a correlated one-dimensional band. Our results are based on exact (N = 8) and quadruple-configuration interaction (N = 10) finite chain calculations, and therefore, long range interactions (as would occur in PPP models) which add to the inherent discreteness of the short chain energies, are neglected.

THE NONINTERACTING LIMIT

Even for $U = V = 0$, the half-filled band is a semiconductor for nonzero δ. In Fig. 1(a) we show all one-electron excitations from the ground state, while in Fig. 1(b) we show the set of two-electron excitations that have nonzero dipole couplings with the $1B_u$. Intraband excitations from the $1B_u$ that are also one-electron states are relevant for nonresonant nonlinear optics, but are not of interest here. The corresponding continuum states are shown within a total energy scheme in Fig. 1(c). While the overall two-electron continuum includes states other than those shown in Fig. 1(b), the latter contains the edge of the two-electron continuum. Thus the two-electron continuum begins exactly at $2 \times E(1B_u)$, where $E(1B_u)$ is the energy of the $1B_u$ state. The ground state absorption, and the absorption from the $1B_u$ to the two-electron continuum are identical, and are shown schematically in Fig. 1(d). The absorption profile of the one-electron excitation is different upon exciton formation. The exciton acquires a very large oscillator strength, while the strength of the transition to the continuum is diminished. Biexciton formation would require similar splitting off of states from the two-electron continuum. The nature of the absorption from the $1B_u$ in such a case has not been discussed previously.

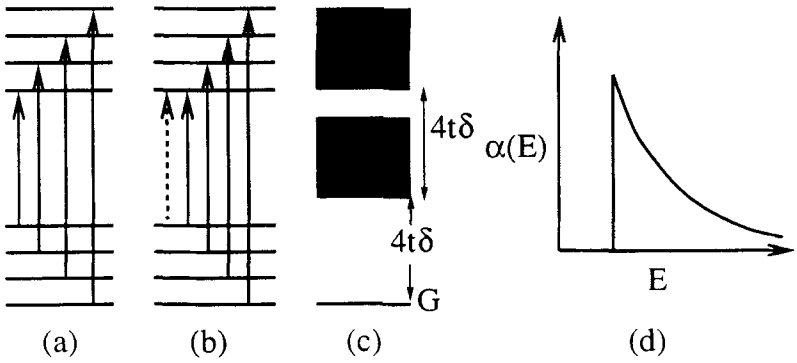

FIGURE 1(a) Excitations from the ground state; (b) excitations from the $1B_u$; the dashed arrow corresponds to the excitation from the ground state to the $1B_u$; (c) the total energies of the one- and two-electron continuua in the noninteracting rigid band; (d) ground state absorption and absorption from the $1B_u$, which are identical in the noninteracting rigid band.

NONZERO COULOMB INTERACTION

It is now convenient to describe the excitations within a configuration space picture[8]. The ground state is approximated by the antiferromagnetic configuration, and all dipole-allowed optical processes correspond to nearest neighbor CT. CT processes most relevant for us are shown in Fig. 2. The exciton consists of an ion pair, i.e., neighboring sites that are doubly occupied by electrons and that are empty. The mA_g is an even parity exciton in which the charge-separation is larger than that in the $1B_u$ exciton, while the nB_u is the threshold of the one-electron continuum. The $2A_g$ is a spin-excitation in this strongly correlated limit. The $1B_u$, the mA_g and the nB_u determine the magnitude of third order optical nonlinearity almost entirely. The contributions of states like the $2A_g$ to third order nonlinearity is negligible in the long chain limit because of a cancellation[9]. This description gives a simple mechanical picture for third order optical nonlinearity, and predicts three distinct resonances in highly resolved third harmonic generation spectra, two three-photon resonances to the $1B_u$ and the nB_u, and a two-photon resonance to the mA_g. The actual observation of three resonances[3] in the polydiacetylenes (PDAs), a crystalline polysilane, and even in cis-polyacetylene confirms that the strongly correlated picture of Fig. 2 is applicable to realistic correlation parameters. Our motivation here is to numerically confirm the existence of stable biexcitons for realistic Coulomb parameters.

The strong-coupling biexciton in Fig. 2 is the lowest two-electron excitation and consists of two neighboring ion pairs. The two-electron continuum states are not shown in Fig. 2. Within Eq. (1), the lowest two-electron continuum states consist of separated excitons, and as in Fig. 1(b), this set of two-electron excitations also have nonzero dipole coupling with the $1B_u$. The threshold of the two-electron continuum is still at $2 \times E(1B_u)$. Stable biexciton for realistic interactions would imply an energy gap between the lowest two-electron excitation and the two-electron continuum for such interactions.

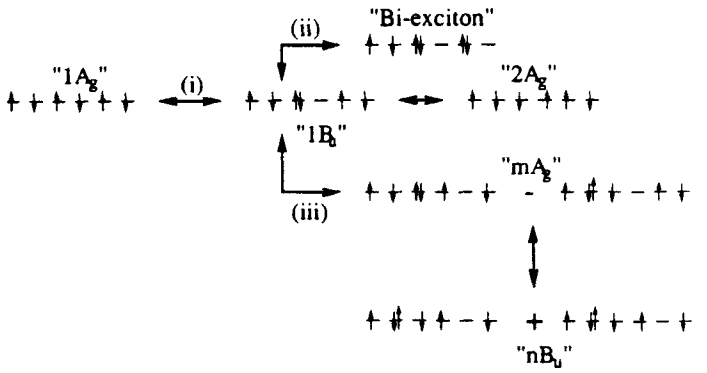

FIGURE 2 Optical processes in the strong coupling (large U,V) limit (see text). In addition to the strong coupling biexciton, absorption from the $1B_u$ will also give separated excitons that form the two-electron continuum.

STABLE BIEXCITONS, NUMERICAL RESULTS

The direct demonstration of stable biexcitons within Eq.(1) is exceedingly difficult, if not impossible. Demonstration of a biexciton requires the simultaneous determination of the two-electron continuum. Thus the ideal calculation must include configuration interaction with at least all doubly excited configurations (double-CI, or DCI) for a long chain, since only a long chain can have true continuua. However, DCI calculations are currently not possible for long chains. Such problems do not arise in the demonstration of the one-electron exciton, since single-CI calculations[10], which can be carried out for long chains, suffice in this case. The only alternative is then to perform exact short chain calculations, for which energy states are necessarily discrete for realistic interaction parameters and continuum states do not exist. Even worse, because of this discreteness, the very identification of the lowest two-electron excitation from energies alone is difficult. We therefore adopt the same procedure that was previously used to identify the one-electron continuum from exact finite chain calculations. We monitor *wavefunctions*, rather than energies, with the understanding that the wavefunction characters of the exciton, one-electron continuum, biexciton, and two-electron continuum have already formed in short chains. As the chain length increases, more and more states fill in the energy gaps, but there is no fundamental change in wavefunction characters.

Strong Coulomb interactions

For illustration only, we start with very strong Coulomb interactions $U = 50, V = 15$ (in units of t). In Fig. 3 we show the exact energy levels for $N = 8$ for this case, upto the two-electron continuum. The spin-wave states(containing the $2A_g$), the exciton "band" (containing both the $1B_u$ and the mA_g) at energy $U - V$, and the one-electron continuum (containing the nB_u), centered at energy U, have been previously discussed in the context of nonresonant optical nonlinearity[8]. The biexciton "band" consists of states at

$2U - 3V$ in Fig. 3. The spectrum of strongly correlated mixed-stack CT solids[5] resembles that in Fig. 3 (with the only difference that the spin-wave states are absent in these charge density wave systems), indicating a basic universality in one-dimensional physics. For realistic Coulomb correlations, the two continuaa cannot be detected from energies, and wavefunction analysis becomes necessary.

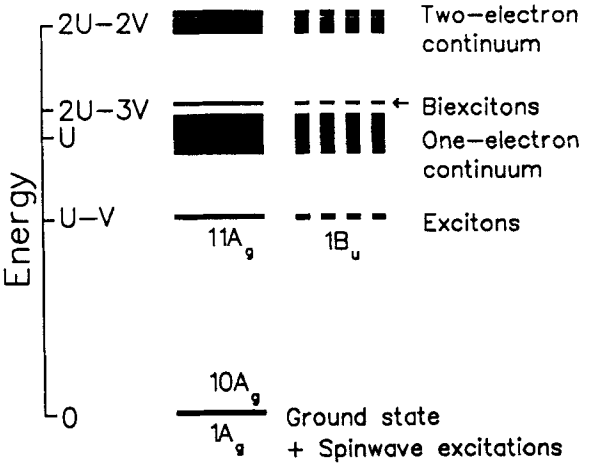

FIGURE 3 Total energies of the N = 8 finite chain for $U = 50, V = 15$. The A_g states are on the left, the B_u states on the right. The $11A_g$ is slightly above the $1B_u$ and is the mA_g for these parameters and chain length. The one- and two-electron continuaa are centered at U and $2U - 2V$, while the biexciton states occur at $2U - 3V$. The relatively smaller width of the two-electron continuum, compared to the one-electron continuum is a finite size effect.

Realistic Coulomb Interactions

We have chosen $U = 3, V = 1$ as realistic parameters for π-conjugated polymers. As will be obvious from our discussion below, the precise values of the parameters are irrelevant. The wavefunction analysis that is now necessary to prove stable biexcitons follows from a simple physical argument. The lowest two-electron states within the interacting models consist of two excitons. Biexciton formation requires that the second exciton is formed in the immediate vicinity of the first exciton, and as shown in Fig. 4(a), there are then only two possible "spots" for the formation of the second exciton. On the other hand, two-electron continuum states are reached by creating the second exciton anywhere else on the chain. Thus from a "density of states" argument we expect a relatively smaller dipole coupling between the $1B_u$ and the biexciton than between the $1B_u$ and the threshold state of the two-electron continuum. Conversely, smaller dipole moment between the $1B_u$ and the lowest two-electron excitation is a definite signature of bound exciton. In Fig. 4(b) we give a schematic of the two-electron excitation based on this argument. Note that the predicted behavior is now *exactly opposite* to that of ground state absorption, where the exciton acquires a *larger* transition dipole moment with the ground state as the exciton binding energy increases.

As discussed above, identification of the lowest two-electron excitation itself is difficult for realistic δ. In order to overcome this problem, we start our calculations with very large δ ($\delta = 0.5$). For small Coulomb interactions, such

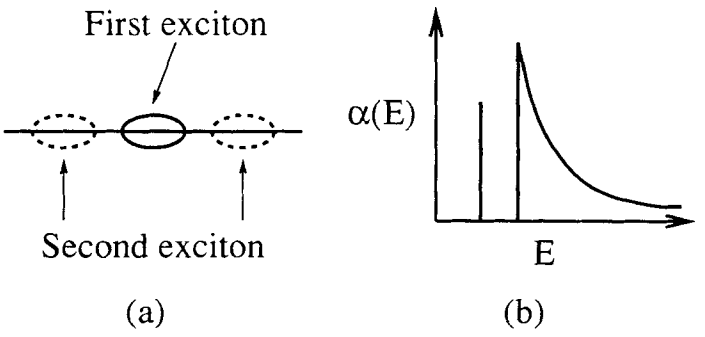

FIGURE 4(a) Location of the second exciton (one of two dashed ellipses), relative to the first (solid ellipse) in a biexciton. In a two-electron continuum state the second exciton occurs at arbitrary distance from the first. (b) Schematic of the absorption from the $1B_u$ to the two-electron states in case of biexciton formation.

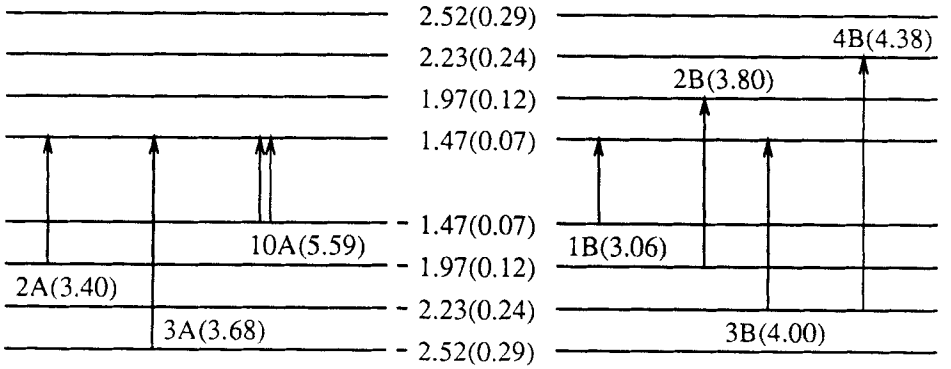

FIGURE 5 Decomposition of exact N = 8 total energies (in units of t) into approximate MO energies for U = 3, V = 1, $\delta = 0.1$. The total energies are given in parenthesis against representative even and odd excitations, while the numbers against the MOs are their approximate single-particle energies, with the error bars included. The vertical arrows denote the excitations within the MO scheme. The $10A_g$ is obtained by exciting two electrons across the gap, and is the lowest two-electron excitation.

large δ is close to the band limit, and all total energy states can be decomposed into *approximate* molecular orbital (MO) energies, as is shown in Fig. 5. This allows us to clearly classify total energy states as one- vs. two-electron excitations and also to identify the lowest two-electron excitation. From the exact energy eigenstates we determine the normalized dipole couplings between all A_g states and the $1B_u$. The normalized dipole couplings as a function of energy for δ=0.5 are shown in Fig. 6(a). The level marked B in the figure is the $10A_g$, the lowest two-electron excitation from Fig. 5. A_g states below B are the one-electron A_g excitations of Fig. 5. Note that the two-electron part of the

spectrum in Fig. 6(a) is almost what is expected for a two-electron continuum in the band limit (see Fig. 1(d)). The occurrence of level B below $2 \times E(1B_u)$ is already suggestive.

We now reduce δ gradually ($\delta = 0.1$ would correspond to the polyacetylenes, while $\delta = 0.2$ - 0.3 would correspond to polymers in which the $2A_g$ occurs above the $1B_u$). These results are summarized in Figs. 6(b) - 6(d). The $2A_g$ in all cases is labelled as 2. In addition we have labelled a higher one-electron A_g state as m. This is the mA_g state of Fig. 2, and has been shown to be the dominant two-photon state relevant for nonresonant nonlinear optics[8]. The slow gradual change in δ allows us to continue to demarcate between one-electron and two-electron excitations. It is clear that the major effect of reducing δ (and thereby increasing the relative Coulomb contribution to the optical gap) is a redistribution of dipole moments with $1B_u$: the relative shifts in energies is small within this range of parameters. There should be no doubt whatsoever that in all cases the levels marked B are the lowest two-electron excitations.

We now discuss the issue of bound biexcitons. The energy difference between the threshold $2 \times E(1B_u)$ of the two-electron continuum and that of the biexciton(if it exists) should increase with increasing Coulomb contribution to the optical gap. The A_g states B in Figs. 6(b) - 6(d) are, however, shifted to above $2 \times E(1B_u)$ at smaller δ. This is because *all* two-electron excitations are shifted to higher energies for small δ and U due to a finite size effect that is easily understandable. With increasing Coulomb interactions (decreasing δ), the ground state gradually becomes more covalent, and the exciton and the biexciton begin to acquire site charges, as shown in Fig. 2. Since these charges avoid the ends of a finite open chain, the biexciton wavefunction with four site charges is effectively "squeezed" more than the exciton with two site charges, and its energy is raised relative to the $1B_u$. Thus the biexciton in a short chain is at relatively high energy for the same reason that the one-electron continuum states occur at relatively high energies in short chains[8]. This finite size effect will continue to be relevant until the Coulomb interactions are large, and strong localization makes the exciton of width one lattice constant, as in Fig. 2. Only for large interactions the biexciton in finite chains occurs below $2 \times E(1B_u$ (see Fig. 3). It is because of the apparent energy discrepancy at small U and V that the criterion of Fig. 4 becomes necessary to prove stable biexcitons. We have discussed in the above that the lowest two-electron excitation is a biexciton provided there exists a higher energy two-electron excitation which has a larger dipole moment with the $1B_u$. Note that this is *exactly* what happens as we proceed from Fig. 6(a) to (d): as the effective Coulomb interaction increases, the dipole coupling between B and the $1B_u$ becomes smaller than that between a higher energy two-electron excitation C and the $1B_u$. This *qualitative* change in the dipole moment profile in the two-electron part of the spectrum is a distinct signature of a bound biexciton. It is also significant that while the absolute energies of B(biexciton) and C(edge of two-electron continuum) are too high, their energy *difference*, does increase with decreasing δ. Thus for realistic δ, we expect stable biexcitons within Eq. (1).

The validity of the wavefunction analysis approach is now demonstrated by examining the relatively strong Coulomb interaction case of $U = 10, V = 3$, and $\delta = 0.1$, where the localization is strong. For such large interactions, the biexciton binding energy is very large and the two-electron continuum begins almost exactly at $2 \times E(1B_u)$. The two-electron spectrum in this case is shown in Fig. 7(a), while the two-electron spectrum of Fig. 6(c) is reproduced in Fig. 7(b). The dipole moment profiles are identical, and are also similar to that in Fig. 4(b). This proves our contentions that, (a) the relatively high energies of B

and C in Figs.6(b) - (d) are finite size effects important in the small correlation case, and (b) the two-electron spectrum should resemble Fig. 4(b) in case of biexciton formation.

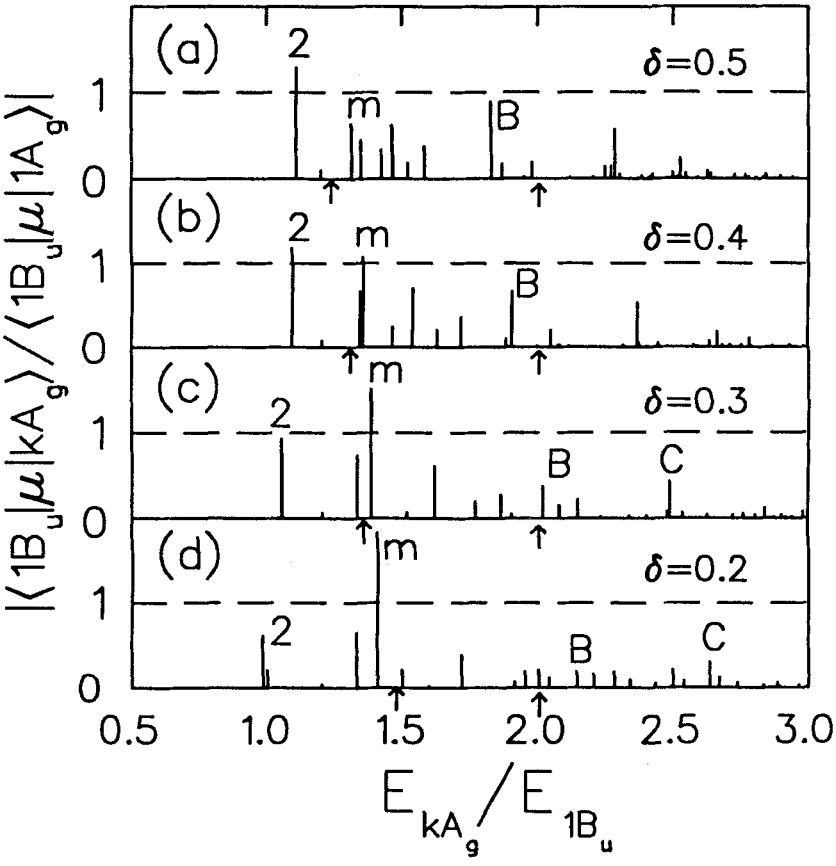

FIGURE 6 Normalized dipole couplings between A_g states and the $1B_u$, plotted against normalized energies, for four different δ but the same correlation parameters, $U = 3, V = 1$. The arrow against the x-axis at normalized energy 2.0 is the threshold of the two-electron continuum in the long chain limit. The levels labelled 2, m and B are the $2A_g$, the mA_g and the biexciton. The assignment of B as the lowest two-electron excitation follows from the continuous tracking of the one- and two-electron excitations as δ is reduced from 0.5 very gradually. The level C, a higher two-electron state, has a larger dipole moment with the $1B_u$ than B at small δ, indicating bound biexciton (see text and Fig. 4). In long chains, the biexciton should occur below $2 \times E(1B_u)$ (see text).

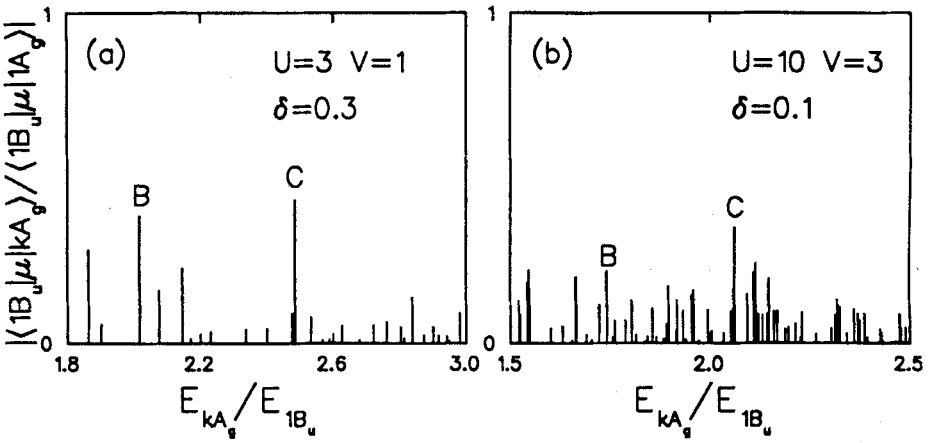

FIGURE 7 Dipole moments between the two-electron states and the $1B_u$ for, (a) U = 3, V = 1, δ = 0.3, and (b) U = 10, V = 3, δ = 0.1. Finite size effects are very small for the strong interactions in (b), and the biexciton B occurs below $2 \times E(1B_u)$, while the two-electron continuum edge C occurs almost exactly at $2 \times E(1B_u)$. In both cases, C has a larger dipole coupling with $1B_u$ than B, proving that the criterion of biexciton stability is valid even when finite size effects are strong (as in (a)).

PHOTOINDUCED ABSORPTION

We expect both the mA_g and the biexciton to be observable in PA experiments at short time delays. The $2A_g$ in most cases is expected to occur too close to the $1B_u$ exciton, while the two-electron continuum states occur in the same energy region where bleaching of the ground state absorption occurs. Based on this argument, together with our experimental colleagues we have recently proposed that the short-time PA at 0.5 eV and at 1.5 eV in PPV correspond to these two transitions from the $1B_u$ exciton[6]. The dynamics of the 0.5 eV and 1.5 eV PA are the same, indicating that they have the same origin. The photoluminiscence (PL) dynamics and the PA dynamics are correlated upto 400 ps, but while there is very little PL beyond 400 ps, PA is essentially unchanged even in the ns time domain. Based on this difference in PL and PA decays in the long time regime, Hsu and collaborators[7,11] have explained PA within a polaron-pair mechanism, whereby the electron or the hole of the exciton migrates to a different chain, and each chain now has a polaron.

The different PL and PA decay rates in the long time domain can, however, be explained within the theoretical picture once relaxation processes neglected in our rigid band calculations are considered. This has been discussed by Leng[12], and will not be repeated here. Rather, we list additional experimental evidence that we believe indicates that the PA is due to absorption from the primary exciton. Firstly, the high energy ps PA is a general phenomenon, and occurs in several other π-conjugated polymers[13,14]. In particular, Kobayashi

et. al. have seen PA at 1.4 eV and 1.8 eV in blue-phase PDAs, in which the exciton occurs at 1.95 eV, and conjugation lengths are truly long. Large side groups in the PDAs should also reduce or eliminate the possibility of interchain electron or hole migration. On the other hand, the exciton binding energy is known to be about 0.5 eV in the PDAs, and the rigid band estimate of biexciton energy as $2 \times E(1B_u)$ minus the exciton binding energy suggests that the 1.4 eV PA is due to biexcitons. The 1.8 eV PA can be due to the edge of the two-electron continuum, assuming that its relaxation energy is more than that of the exciton such that PA becomes observable on the low energy side of the bleaching. Secondly, both the mA_g and the biexciton should be observable in two-photon absorption (TPA), while the mA_g should also be observable in electroabsorption (EA)[8]. Observation of TPA[15] in PPV, as well as EA[6] in MEH-PPV at 0.5 eV above the $1B_u$, supports our assignment of the low energy PA. Following the same argument, we point out that in PDHS-polysilane, PA occurs at the same energies[16] that would be predicted from TPA results[17]. It is also significant that the mechanism of PA, as proposed by the authors of ref. 16, is identical to the one proposed by us. We believe that the occurrence of similar PA in widely different materials and the strong correlation between PA and nonresonant nonlinear optical experiments strongly supports our assignment.

ACKNOWLEDGEMENTS

We acknowledge support from AFOSR grant number F49620-93-1-0199. S.M. acknowledges valuable discussions with Professors N. Peyghambarian (University of Arizona) and Z.V. Vardeny (University of Utah).

REFERENCES

1. G. Weiser, Phys. Rev. B45, 14067 (1992), and references therein.
2. U. Rauscher et al., Phys. Rev. B42, 9830 (1990).
3. S. Mazumdar and F. Guo, J. Chem. Phys., in press (1994).
4. N. Peyghambarian, S.W. Koch and A. Mysyrowicz, Introduction to Semiconductor Optics (Prentice Hall, Englewood Cliffs, (1993).
5. M. Kuwata-Gonokami et al., Nature, 367, 48 (1994).
6. J.M. Leng et al., Phys. Rev. Lett. 72, 156 (1994).
7. J.W.P. Hsu et al., Phys. Rev. B49, 712 (1994).
8. D. Guo et al., Phys. Rev. B48, 1433 (1993); See also, S. Mazumdar et al., Synth. Metals, 55-57, 3881 (1993).
9. F. Guo, D. Guo and S. Mazumdar, Phys. Rev. B, in press (1994).
10. S. Abe, M. Schreiber, W.P. Su, and J. Yu, Phys. Rev. B45, 9432 (1992)
11. See Ming Yan et al. and E.M. Conwell, present proceedings.
12. See J.M. Leng et al., present proceedings
13. T. Kobayashi, Synth. Metals, 50, 565 (1992) and references therein.
14. M.B. Sinclair et al., ibid, 50, 593 (1992).
15. C.J. Baker, O.M. Gelsen and D.D.C. Bradley, Chem. Phys. Lett. 201, 127 (1993).
16. J.R.G. Thorne et al., Chem. Phys. 146, 315 (1990).
17. R.G. Kepler and Z.G. Soos, Phys. Rev. B43, 12530 (1991).